ADVANCED MATERIALS INTERFACES
Open Access
www.advmatinterfaces.de

Noise Spectroscopy Analysis of Ion Behavior in Liquid Gate-All-Around Silicon Nanowire Field-Effect Transistor Biosensors

*Yongqiang Zhang, Nazarii Boichuk, Denys Pustovyi, Valeriia Chekubasheva, Hanlin Long, Mykhailo Petrychuk, and Svetlana Vitusevich**

The transport and noise properties of fabricated, high-performance, gate-all-around silicon liquid-gated nanowire field-effect transistor devices are investigated in different concentrations of $MgCl_2$ solutions. The critical concentration of $MgCl_2$ solution for charge inversion at the solid-liquid interface is verified using noise spectroscopy and confirmed using the capacitance-voltage measurement technique. In this study, it is found that the Hooge parameter (α_H) and the equivalent input noise (S_U) can effectively reflect the ion behavior on the surface of the nanowire. Moreover, the noise curves for α_H and S_U indicate two turning points at concentrations of 10^{-4} and 10^{-1} M for a peak and a valley, respectively. The noise transformation is related to the behavior of ions near the solid-liquid interface in solutions with different $MgCl_2$ concentrations is revealed. The results show that noise spectroscopy is a powerful method for monitoring charge dynamic processes in the research field of biosensors.

1. Introduction

Field-effect transistors (FETs) have attracted widespread attention due to their ultrahigh sensitivity, low detection limit, and low-cost fabrication process.[1–5] Different kinds of FET biosensors have been used to detect a variety of diseases (e.g., heart, neurodegenerative, etc.) to protect the health of the human body. The detecting principle of nanowire FET biosensors is based on binding charged biomolecules on the surface of the nanochannel. This results in detectable signals in the form of a threshold voltage shift, which is induced by a change in the electrical potential of the nanochannel surface. A novel approach was recently reported in which a single-trap phenomenon found in a dielectric layer enables an improvement in biosensor performance and enhances device sensitivity.[6,7] The device may employ different bioliquids, such as phosphate-buffered saline (PBS) solution with a main contribution of monovalent ions and $MgCl_2$ solutions with divalent ions as a liquid gate to adjust the surface charge density of the nanowires.[6,8] In order to consider fabricating high-performance, stable FETs, there needs to be a focus on the solid-liquid interface, especially on the charge effect and the dynamic process at the solid-liquid interface.

To date, the detection mechanism of FET biosensors has been considered to be generally similar to the metal oxide semiconductor field-effect transistor, which consists of a drain, a source, a nanowire channel, a dielectric layer, and a liquid gate instead of a metal gate. Close-to-physiological liquids were typically employed for dissolving target-charged biomolecules in order to obtain liquid gates for molecular detections. To analyze the useful signal recorded as a change of potential at the solid-liquid interface, the different concentrations of ions need to be studied. Typically, the positive and negative charges near the solid-liquid interface depend on the pH and the ionic strength of the solution being tested. Kutovyi et al. reported that charged molecules interact with various ions in the electrolyte condition.[7] This causes the oppositely charged ions to attract and similarly charged ions to repel via Coulombic forces. To further investigate the influence of ion composition at the solid-liquid interface in very small concentrations of solutions, it is crucially important to develop recognition transducers for useful electrical signal recording due to the different ions and molecules in biosensor solutions. Therefore, the expansion of biosensor detection principles and the verification of signal registration reliability are issues that are crucial to obtaining high-performance devices.

Charge inversion has recently attracted widespread attention due to its important role in various sensing measurements. Li et al. compared the monovalent ionic and $MgCl_2$ divalent ionic

Y. Zhang, N. Boichuk, D. Pustovyi, V. Chekubasheva, H. Long, M. Petrychuk, S. Vitusevich
Institute of Biological Information Processing, Bioelectronics (IBI-3)
Forschungszentrum Jülich
52425 Jülich, Germany
E-mail: s.vitusevich@fz-juelich.de
Y. Zhang, N. Boichuk, D. Pustovyi, S. Vitusevich
Experimentelle Physik 2
TU Dortmund University
44227 Dortmund, Germany

The ORCID identification number(s) for the author(s) of this article can be found under https://doi.org/10.1002/admi.202300585

DOI: 10.1002/admi.202300585

liquids at the solid-liquid interface in a microfluidic channel and reported charge inversion in a microfluidic channel with a small diameter.[9] Moreover, the contribution of counter ions[10] should be considered with respect to influencing the compensation of surface charge at the solid-liquid interface. Although the charge inversion phenomenon was observed in previous experiments, numerous discussions concerning its origin can be found in the literature. Authors of works[11,12] suggest that the ion–ion correlation likely explains the inversion effect. It is also suggested that the site-binding model, which is useful for calculating theoretical surface charge densities, might explain the mechanism of ion binding to surface groups of the dielectric layer.[13] Several capacitors connected in series are considered, including the formation of a double-layer capacitance and the Helmholtz planes at the solid-liquid interface during ion detection. It includes a double layer where negative (positive) ions reach the surface as the first layer, and the positive (negative) ions form a separate second layer. With increasing distance from the solid-liquid interface, the potential decreases due to the diffusion process and the change in ion concentration.

The sensing ability was typically a critical factor in evaluating the performance of the device. To obtain high-sensitivity FETs for pH detection, an additional coating layer covering the gate oxide layer can be applied to reduce the interference of other ions in high-concentration electrolytes. Wipf et al. employed a thin gold film to modify nanowires in order to functionalize the surface for the detection of specific analytes, in which a response to Na^+ ions reached ≈−44 mV per decade in NaCl solution.[14] Sivakumarasamy et al. fabricated a special 25 nm silicon nanostructure without implementing a selective layer onto the SiO_2 layer in order to study the ion-surface interaction.[15] They analyzed Na^+, K^+, Ca^{2+}, and Mg^{2+} ions originating from blood serum using these transistors and suggested that strain was a possible mechanism responsible for the selectivity. Therefore, the effect of ion interactions with the substrate of semiconductor transistor structures still needs to be investigated for different biochemical sensor applications.

In previous studies, it was reported that the charge states formed near the nanowire surface can significantly influence the transport properties and effectively enhance the sensitivity of the device. Guo et al. considered the ion-related phenomena in two-layer silicon nanowire FETs and reported the space-charge-limited current (SCLC) effect in liquid-gated nanochannels.[16] As it is known, the SCLC is a very useful method for the analysis of solid surface trapping processes. Numerous studies found that the SCLC plays a very important role in the redistribution of carriers in nanochannels, especially in the nanowire structures of GaAs, CdS, GaN, InAs, and ZnO.[17–22]

In addition, the systematic study of charge inversion with multivalent ions was reported by Lemay et al. in 2005.[23] They adopted the atomic force spectroscopy (AFM) technique to directly test charge inversion via the dielectric constant and density of surface charge of different liquids, which demonstrated the changes of critical concentration in several conditions with different complex permittivities. The authors underlined that not only physical effects, but also biochemical phenomena should be considered at the solid-liquid interface. In short, research on the double-layer capacitance close to the nanochannel surface is urgently required, especially since the FET devices have potential applications in medical diagnostics.

It is important to note that the capacitance-voltage (*C*–*V*) characterization represents a good way of analyzing what occurs with the diffuse double-layer capacitance in the solid/solution interface region. Furthermore, numerous studies have confirmed that the potential decreases as the distance from the surface increases in the double-layer capacitance. Meanwhile, Christensen et al. highlighted the different shapes of *C*–*V* curves in various concentrations of KCl solutions, revealing a definite relationship between the double-layer capacitance and ion behavior near this interface.[24] Moreover, Hlukhova et al. utilized the electrolyte–insulator–semiconductor (EIS) structure covered with a functional layer to enhance the selectivity and sensitivity of testing different concentrations of antigen by employing the *C*–*V* characteristic as an effective method.[25] The *C*–*V* measurement thus has the potential to be used for studying the behavior of various ions at the solid/liquid interface of a nanochannel.

Despite the progress in the presentations of models proposed to explain the effect of inversion at the solid-liquid interface, the development of methods for the direct monitoring of processes at the interface is an important aspect. It was recently shown that noise spectroscopy is a highly sensitive method for studying dynamic processes in nanodevices and hybrid materials. It should be noted that fluctuation processes and the dimensionless Hooge parameter[26–28] allow a quantitative comparison of the intensity of dynamic processes that can take place in different materials and devices. At the same time, the studies of the Hooge parameters in cases involving the participation of divalent ions in the dynamic processes occurring on the solid-liquid interface with the possible involvement of the inversion effect at the interface have not been reported in the literature.

In this work, we fabricated and studied properties of gate-all-around (GAA) nanowire FETs with a 20 nm SiO_2 dielectric layer to analyze Mg^{2+} ion behavior at a solid-liquid interface in a concentration range from 10^{-6} M to 1 M. It should be emphasized that the $MgCl_2$ solutions play an important role in the human body. They participate in many enzymatic reactions, DNA folding, and its concentration reflects the health state of the gastrointestinal tract. We demonstrated a small threshold voltage (V_{TH}) value range between −0.2 and −0.3 V of the transistors with several *I*–*V* curves in different concentrations of $MgCl_2$. Moreover, noise spectroscopy was applied to analyze ion behavior at the solid/liquid interface. The important Hooge parameter (α_H) and the equivalent input noise (S_U) were analyzed to study the contribution of surface properties. Initially, both α_H and the spectral density of S_U decrease with an increasing concentration of $MgCl_2$, reaching their minimum values at 10^{-4} M and consequently obtaining their maximum values at $\approx 10^{-1}$ M. It was demonstrated that the fluctuation of noise originates from ion behavior on the nanowire surface and is consistent with the results obtained using the *C*–*V* measurement technique.

2. Results and Discussion

The schematic design of the LG GAA FET with Si substrate/buried SiO_2/Si nanowire channel/gate SiO_2 is shown in **Figure 1**A. Atomically flat 2 μm long nanowire channels were

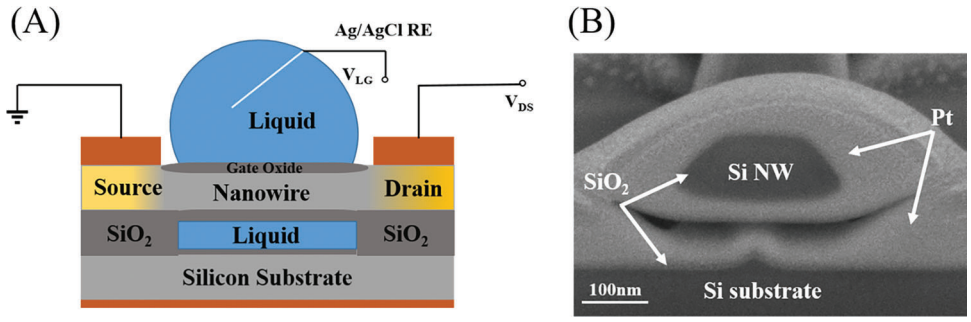

Figure 1. A) Schematic illustration of the gate-all-around Si nanowire FET. B) SEM image of a nanowire cross-section, obtained using the focused ion beam (FIB) cut technique (with the Pt protection layer deposited on the nanowire).

fabricated from low doping concentration (≈10^{15} cm^{-3}) silicon layer of silicon on insulator wafer (SOI). The SEM image of nanowire cross-section was obtained after a nanowire cut using focused ion beam (FIB) cut technology Figure 1B. One can see that the nanowire has trapezoidal cross-section with a top- and bottom-base widths of 100 and 200 nm, respectively. The silicon nanowire is protected by 20 nm thin SiO_2 layer from direct contacting with a liquid. We focus on the transport and noise properties of fabricated devices in different $MgCl_2$ solutions under different liquid gate voltage (V_{LG}) and drain-source voltage (V_{DS}) values. Here, the GAA structures were fabricated by wet etching instead of reactive ion etching (RIE) to form a planar nanowire structure. The electrical properties of four devices demonstrate the same behavior. As expected, the transistor with the GAA shows a better pH response value of ≈61 mV pH^{-1} than our previous report of ≈54 mV pH^{-1},[7] and the corresponding shift of transfer current–voltage (I–V) curves is shown in Figure S1A,B (Supporting Information). The increased sensitivity indicates that the surface–volume ratio of the GAA transistor was larger than that of the planar structure device. This means that more proton charges reach the surface and change the potential.[29]

The I–V curves for the GAA structure sensor with different concentrations of $MgCl_2$ solutions in a range from 10^{-6} to 1 M were measured using in house-developed system. It should be noted, that the leakage current was negligibly small at the level of nA currents. Series of transistors with a length of 2 µm and with different widths (100, 150, 200, and 300 nm) were studied. The results of studying several transistors with differently sized channels demonstrate the same trend. Transfer characteristics I_{DS}–V_{LG} of liquid-gated NW FET measured in $MgCl_2$ solutions at V_{DS} = −100 mV for the nanowire channel with a width of 100 nm and a length of 2 µm are shown in **Figure 2**A. It should be noted that the behavior of transfer characteristics is typical for high-quality NW FET structures and is in a good agreement with common description of I_{DS} as a function of V_{LG} using the following relations:

$$I_{DS} = \begin{cases} 0, & V_{LG} \le V_{TH}; \\ C_{ox}\mu\frac{W}{L}\left[\left(V_{LG}-V_{TH}\right)V_{DS}-\frac{1}{2}V_{DS}^2\right], & V_{LG} > V_{TH}, V_{DS} \le V_{LG}-V_{TH}; \\ C_{ox}\mu\frac{W}{L}\left[\left(V_{LG}-V_{TH}\right)V_{DS}-\frac{1}{2}V_{DS}^2\right], & V_{LG} > V_{TH}, V_{DS} > V_{LG}-V_{TH} \end{cases} \quad (1)$$

where V_{TH} is the threshold voltage, μ is the hole mobility, C_{ox} is the capacitance of gate oxide layer, λ is the nanochannel length modulation parameter, V_{DSsat} is the saturation V_{DS}, and W and L are the width and length of the nanowire, respectively.

It can be seen that the I_{DS} decreases with an increase in the concentration of $MgCl_2$. In fact, the solid-liquid interface changes when positive Mg^{2+} arrives on the nanowire surface. As the concentration of $MgCl_2$ solutions increases, the density of ions in the solution also increases. This results in change of interaction processes of solution ions with the gate oxide surface, leading to the changes in the surface charge density and the electrical potential at the Si/SiO_2 interface. In turn, this affects the

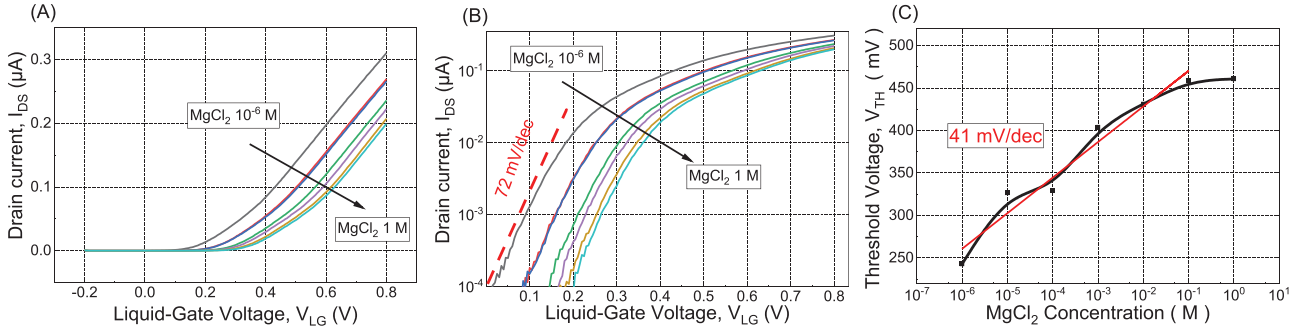

Figure 2. A) Typical transfer characteristics of I_{DS}–V_{LG} for a GAA nanowire FET with a length of 2 µm and a width of 100 nm, measured in different concentrations of $MgCl_2$ solutions at V_{DS} = −100 mV. B) The transfer I_{DS}–V_{LG} curves from (A), shown in semilogarithmic scale. C) The V_{TH} extracted from (A) as a function of concentration in $MgCl_2$ solutions.

channel conductance and the flow of drain current. Figure 2B shows transfer characteristics in semi logarithmic scale typical for field effect transistors, demonstrating effective control of current in the nano-channel through the application of a liquid gate voltage. The subthreshold slope is estimated to be ≈72 mV dec^{-1} for all I–V curves of the transistor. Mobility of holes in GAA NW FET was estimated to be $\mu_p = 150$ cm^2 V^{-1} s^{-1} using equation for long-channel FETs at low drain-source voltage.[30] This value reflects the high-quality of liquid-gated nanowire devices. It should be noted, that the contact resistance, estimated by using transmission line model,[31] has a negligibly small value (≈4 kΩ, after the rapid thermal annealing), corresponding to ≈1.2% of the total resistance of a GAA FET.

Figure 2C shows the threshold voltage (V_{TH}) values, reflecting surface potential change of the sensor as a function of molar ion concentration measured in the range of 10^{-6} M–10^{0} M, which is in the same range as the prior publication.[16] The dependence reflects small variations from the linearly approximated part in the range of 10^{-6} M–10^{-1} M, demonstrating V_{TH} sensor sensitivity ≈41 mV decade^{-1} with a tendency for saturation when the $MgCl_2$ concentration reaches ≈0.1 M.

In general, the concentration of ions in the $MgCl_2$ solution determines the number of ions that can be absorbed on the gate oxide surface. Higher concentrations of ions will lead to a stronger modulation of the surface charge and thus a more significant shift in the V_{TH}. The dependence V_{TH} as a function of $MgCl_2$ concentration can be described using the following equation:

$$V_{TH} = V_{DS} - \psi_0\left(c_{MgCl2}\right) + \chi^{lq} - \frac{W_{si}}{q} - \frac{Q_{ox} + Q_{ss}}{C_{ox}} \quad (2)$$

where $\psi_0(c_{MgCl2})$ is the surface potential modulated by charge state change in $MgCl_2$ solutions of different concentrations, χ^{lq} is the surface dipole potential of the solution, W_{si} is the width of nanowire, q is the elementary charge, Q_{ox} is the fixed charges in the oxide, Q_{ss} is the fixed charges at the oxide-Si interface, and C_{ox} is the capacitance of gate oxide layer.

As the size of the nanowire scales down, conventional electrical characterization is subject to non-negligible signal fluctuations originating not only from inside the transistor (built-in potential, mobility degradation, hot-carrier effect, etc.), but also outside, that is from the media surrounding the transistor. At the same time, on the nanoscale, measurements of electrical noise and fluctuations become powerful and a useful way of accurately extracting valuable signals from the nanodevice being tested.[7,8,32,33] The most common component of the main noise spectrum of any device structure is known to be $1/f$ flicker noise. In the case of structures containing semiconductor and dielectric materials, the flicker noise is usually caused by the interaction between charge carriers and traps at the Si/SiO_2 interface. It should be noted that carrier exchanges between the nanowire channel and the dielectric layer result in surface potential fluctuations, which influence the I_{DS} current flowing through the nanowire channel. Meanwhile, other noise signals also appear in GAA FETs, especially when the sensor is measured with an applied liquid-gate voltage, V_{LG}, in different chemical solutions. In the liquid environment, the noise signals result from the charge carrier exchange at the solid-liquid interface.[34] Therefore, the α_H and S_U were used to analyze the noise properties of the FET.

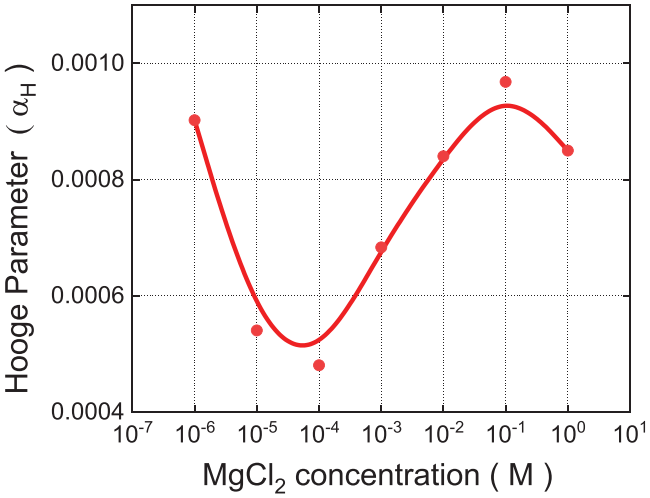

Figure 3. Hooge parameter at 10 Hz extracted from the noise spectrum measured for a GAA NW FET with a length of 2 µm and a width of 100 nm at VLG = −0.4 V, VDS = −20 mV, frequency of 10 Hz in different concentrations of $MgCl_2$ solution. The solid red curve is used as a visual guideline.

The dimensionless Hooge parameter α_H is an important indicator for assessing the performance of the transistor. Its value may usually change between 10^{-2} and 10^{-6}. All data points shown in **Figure 3** are below 10^{-3}, which demonstrates a high-quality device and is in good agreement with previously reported values.[16,31,35] Here, we used α_H parameters obtained for different $MgCl_2$ concentrations at constant voltages: $V_{DS} = -20$ mV and $V_{LG} = -0.4$ V to further study the noise properties of GAA FETs as a function of the concentration. It can be seen that α_H decreases as the concentration increases, reaching its minimum value at a concentration of 10^{-4} M $MgCl_2$. After this level of concentration, α_H starts to increase whereas the maximum value of 9.7×10^{-4} was obtained at a solution concentration of 10^{-1} M followed by a decrease of α_H. In contrast to monovalent ions (e.g., K^+ and Na^+), the divalent ions of Mg^{2+} may exhibit a charge inversion phenomenon at the solid-liquid interface[26] in the microfluid filled with a solution. We registered this effect for GAA FET devices filled with the $MgCl_2$ solutions of medium concentrations, revealed as a transformation region (Figure 3) between low and high-concentration solutions.

Two distinct parts were identified in solutions of $MgCl_2$ with varying concentrations: the conductivity changes slightly at low concentrations. It increases proportionally at higher concentrations. The critical concentration found in the 10^{-4} M $MgCl_2$ solution can be explained by considering the ion composition in the liquid near the solid-liquid interface. The surface charge processes clearly have a major influence on the noise fluctuation of GAA FETs when the concentration of $MgCl_2$ is smaller than the critical concentration, which is the case with almost no charge inversion phenomenon occurring on the surface of the solid. After the critical concentration, which also corresponds with the case of the concentration-dependent conductivity, the conductivity of divalent Mg^{2+} increases. This can explain the valley at a solution concentration of 10^{-4} M in Figure 3. We observed an interesting

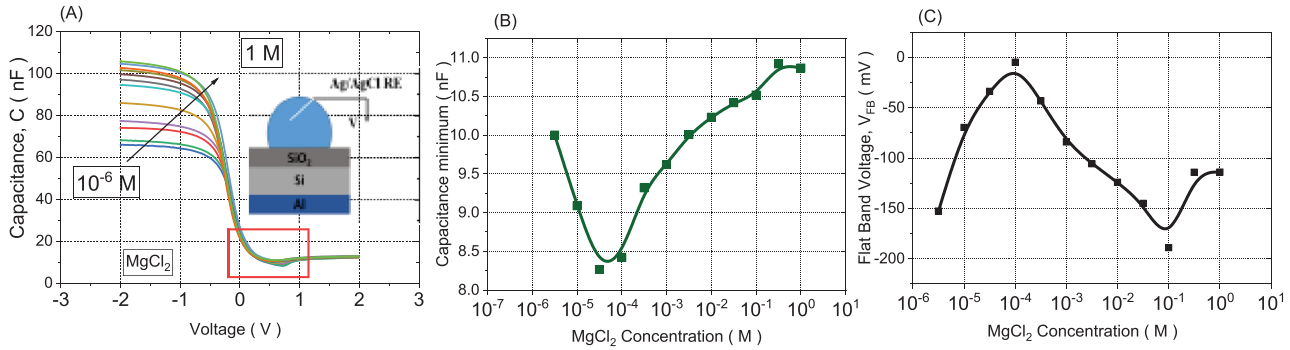

Figure 4. A) Typical *C–V* dependencies for different concentrations of $MgCl_2$. The bottom of the left insert presents the structure of *C–V* samples. B) The minimum value of capacitance in a voltage range between 0–1 V. The data are extracted from the red rectangular area from (A). C) The V_{FB} as a function of $MgCl_2$ concentration.

phenomenon, which was that the α_H reaches its peak value in 10^{-1} M $MgCl_2$ due to the decrease in $MgCl_2$ conductivity at a high concentration range.

We performed the corresponding capacitance measurements of $MgCl_2$, which are in good agreement with this trend. To further understand what occurs in the double-layer capacitance, the flat structure sample Al/Si/20 nm SiO_2 was investigated using capacitance measurements (*C–V*) in different concentrations of $MgCl_2$ solutions with a frequency of 1000 Hz, as shown in **Figure 4**A. The shift was observed in all *C–V* curves as a function of $MgCl_2$ concentration. Moreover, the minimum value of the capacitance (revealed as a valley in a *C–V* curve) was analyzed to be found at a voltage range of 0–1 V, as presented in Figure 4B. The dependence demonstrates the same trend as the dimensionless Hooge parameter Figure 3. The results effectively confirm the charge inversion phenomenon at the solid-liquid interface and support the mechanism of correlations in solutions with charged ions. Subsequently, Figure 4C shows the flat-band voltage (V_{FB}) variating between 0 and −200 mV, extracted from the corresponding *C–V* curves using the Mott–Schottky plot, that is by finding the intersection of the linear part of ($1/C^2$) dependence with the voltage axis. The figure clearly exhibited two characteristic points at concentrations of 10^{-4} and 10^{-1} M. It should be emphasized that at a concentration of 10^{-4} M, the flat-band voltage is almost at zero voltage. This also reflects the strong correlation between positive and negative contributors near the interface, resulting in the low value of the dimensionless Hooge parameter. It should be underlined that registered behavior in threshold voltage (Figure 4C) demonstrates good correlation with data obtained for dimensionless Hooge parameter (Figure 3).

To further investigate the charge inversion phenomenon that occurs at the nanowire channel-fluid interface, we considered the behavior of Mg and Cl ions in the electrolyte. In general, when a charged molecule is exposed to a liquid environment with different ions, then the Coulombic force has an effect on the interaction between the charged ion and oppositely charged ions (counterions) from the electrolyte.[7] Initially, adsorbed ions are repelled when a divalent ion reaches the neutral surface, resulting in a correlation hole effect.[11] Therefore, the behavior of the ions at the surface causes a negative chemical potential due to attracting additional counterions to the surface. This proves that charge inversion behavior takes place at a critical concentration of 10^{-4} M. Different stages of the change in charge states are schematically shown in **Figure 5**A–D.

For low concentration of $MgCl_2$ solution the potential decreases monotonously (Figure 5B) similar as in the case of monovalent ionic solutions. However, with increase of concentration the contribution of counter ions[10] results in neutralization of surface charge (Figure 5C) followed by inversion of surface potential (Figure 5D) with reversible charge change on the surface of NW channel. Such charge inversion was reported for $MgCl_2$ solutions studied in microfluidic channels[9] of small diameter. The potential redistribution is not monotonous with increase of distance from solid-liquid interface of GAA FET followed by decreasing tail due to the diffusion of ions.

To analyze the dielectric layer-liquid interface, the equivalent input noise S_U was calculated. The presence of ions causes a significant increase in input-referred noise. There are some subtle differences compared to the McWhorter model[32] caused by the ion dynamic process from the solution side to reach the transistor surface. It should be noted that the influence of V_{DS} on input-referred noise was negligible during this process. Typically, measurable fluctuations of current in the biosensor channel are caused by the small flow of ions. In our prior experiments, the amplitude and behavior of the input-referred noise increased in the bioliquid of troponin molecules, further validating ion kinetic change.[7] Meanwhile, we found that the level of noise slightly relates to the concentration of ions in a liquid environment.[36] **Figure 6** shows that the S_U decreases with an increase of V_{LG} in 10^{-3} M $MgCl_2$ at a measurement condition of $V_{DS} = -20$ mV. The decreasing trend of S_U reflects the fact that the additional V_{LG} can effectively control the behavior of ions in the vicinity of the nanochannel surface. It means that charged ions attaching to the surface of the nanowire not only influence surface potential but also change the kinetics of ions at the solid-liquid interface. Therefore, it can be concluded that the sensitivity of noise characteristics can be used to analyze the dynamic process of ions in the measured solution, promoting the amplification of the useful signal in the nanochannel with respect to the pure current characterization method. Detailed information on equations can be found in the statistical analysis section below.

The charge inversion phenomenon in the critical concentration at the solid-liquid interface discussed above can also be confirmed in the noise spectra presented in **Figure 7**. The similar

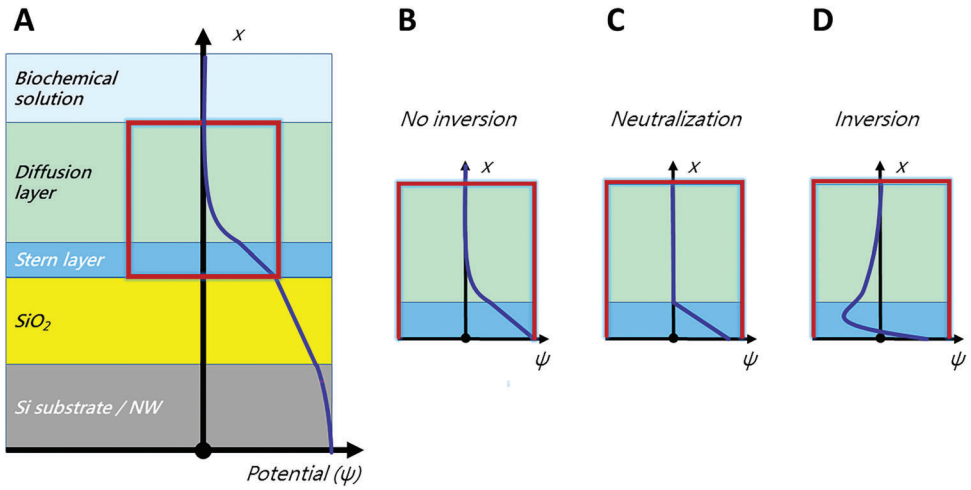

Figure 5. A) Schematic presentation of potential distribution at solid-liquid interface for Si/SiO_2/liquid structures, presented in both Si NW FETs and liquid-gated capacitance-voltage flat structures according to the formation of the electric double layer and the diffusion layer in the liquid being studied. In the case of divalent $MgCl_2$ solutions, three different cases should be considered: B) no inversion, C) neutralization, and D) inversion of the charge state at the solid-liquid interface.

tendency is obtained for frequency dependencies of S_U measured in the same condition $V_{LG} = -0.4$ V and the range of $MgCl_2$ concentration for two values of V_{DS}: A) −20 mV and B) −50 mV. It can be easily seen that in both Figure 7A,B, the noise level of S_U is about the same magnitude between 10^{-9} and 10^{-7} V^2 Hz^{-1} at frequencies <10 Hz. Furthermore, with an increase in the concentration of $MgCl_2$, the intensity of S_U first decreases in a range from 10^{-6} to 10^{-4} M and then increases from 10^{-4} to 10^{-1} M, followed by another subsequent decrease. As expected, the minimum and maximum values of S_U occur in $MgCl_2$ concentrations of 10^{-4} and 10^{-1} M, respectively. This can be reasonably explained by the charge inversion in the critical concentration at the interface mentioned before. We also compared the fluctuation of S_U at different values of V_{DS} and found that at small voltages, the noise spectra are more prone to external signal interference, especially in the frequency range of 100–1000 Hz. The valuable signal at small V_{DS} can be extracted by subtracting the thermal noise values, which dominate at high frequencies (Equation (3) in Section "Statistical Analysis" below: $S_\nu(f > 1\text{kHz}) \approx 4KTR_{eq}$).

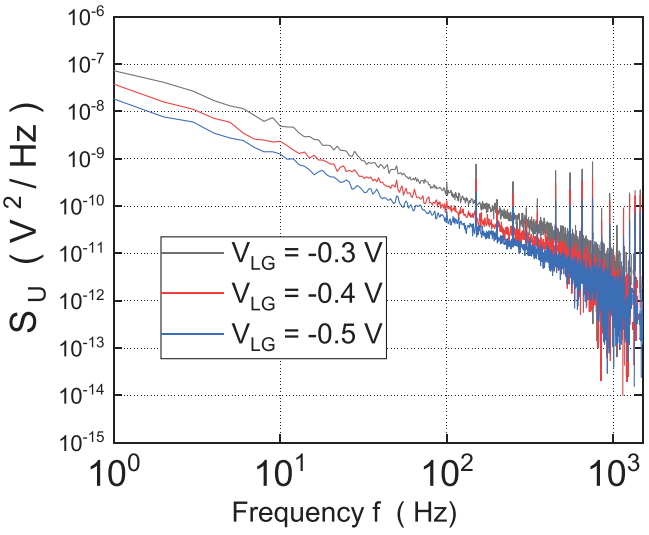

Figure 6. The spectra of the equivalent input noise S_U in the 10^{-3} M concentration of $MgCl_2$ solutions with different V_{LG} at a measurement condition of $V_{DS} = -20$ mV.

To study the behavior of the ions at the solid-liquid interface, the level of noise at 10 Hz points was extracted from the spectra of S_U. **Figure 8**A presents the curves of S_U at 10 Hz with different V_{LG} voltages, labeled as −0.3, −0.4, and −0.5 V, respectively. All curves have two turning points at concentrations of 10^{-4} and 10^{-1} M, revealing the conductivity change of the divalent Mg^{2+} ion at critical concentration, as discussed above. However, the S_U changes significantly with the increase of the V_{LG} voltage. This can be reasonably explained by the ion mobility decreasing due to Coulombic forces pushing ions to the solid-liquid interface by an applied gate voltage on the surface of the nanowire. An interesting phenomenon is shown in Figure 8B (dependence of S_U values on V_{LG} in all concentrations of $MgCl_2$ solutions). It convincingly demonstrates that S_U decreases with increasing V_{LG}, which reflects the fact that the interaction processes can be controlled by surface Coulombic forces.

The equivalent input noise S_U recalculated from the originally measured noise spectra is dependent on the overdrive voltage V_{LG}–V_{TH} in different $MgCl_2$ solutions (**Figure 9**).

One can see that S_U intensities demonstrate a strong dependence and follow the decreasing trend with increasing overdrive voltage. It cannot be explained by fluctuations due to traps in SiO_2 layer, because in case the channel noise is determined by charge fluctuations at the $Si\text{-}SiO_2$ interface, the value of S_U does not change.[37] Changes in the capacitance of the structure (Figure 4B) also cannot be the reason for the change in S_U by considering the fact that the value of S_U changes by a factor of six, however the capacitance of the structure varies within ±15%. Therefore such S_U (V_{LG}–V_{TH}) dependence is related to charge fluctuations at the Si/electrolyte interface, that is ion concentration fluctuations near the surface of the sub-gate dielectric. As the electric field in the interface layer of the electrolyte increases,

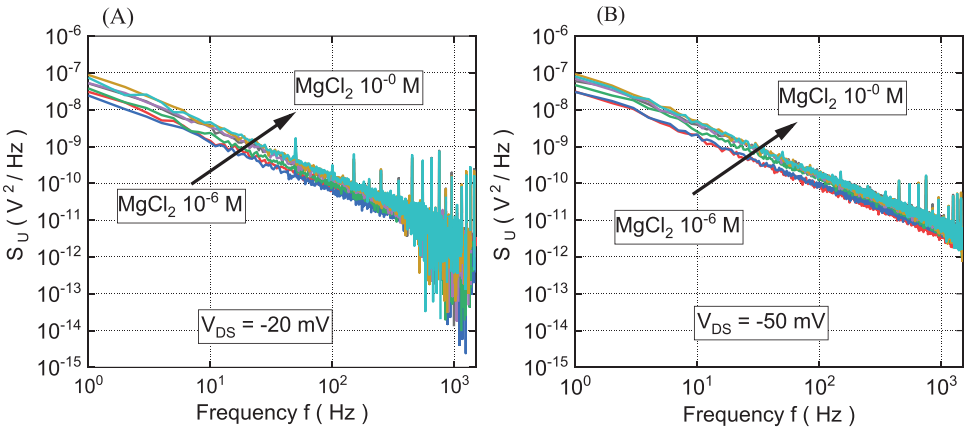

Figure 7. The input-referred noise, S_U, spectra obtained from noise spectra of NW FETs with a nanowire channel of 2 µm in length and 100 nm in width, measured in different $MgCl_2$ solutions: 10^{-6}, 10^{-5}, 10^{-4}, 10^{-3}, 10^{-2}, 10^{-1}, and 1 M at $V_{LG} = -0.4$ V for different drain source voltages: A) $V_{DS} = -20$ mV. B) $V_{DS} = -50$ mV.

the mobility of the ions decreases due to increased interactions in parallel channels, represented by ions and charged channel carriers and, accordingly, the noise caused by the mobile ions also decreases. This behavior is in good agreement with S_U results of the decreasing trend as a function of overdrive voltage when troponin antigen molecules binding on the surface were published in our previous publication.[7] This result indicates that the fluctuations and behavior of S_U in the liquid of charged ions further validates changes in ion kinetics. This noise origin is also confirmed by the strong dependence of the S_U value on the $MgCl_2$ concentration (Figure 8). The noise characteristic is a promising method for investigating ion dynamics and ion–ion correlation on the surface of the dielectric membrane in a bioliquid environment.

3. Conclusion

In summary, the liquid gate-all-around nanowire FET sensors were fabricated to study ion behavior at the interface between a dielectric layer covering a nanowire channel and $MgCl_2$ solutions using electrical and noise characterization methods. A series of noise characteristics demonstrate charge inversion with divalent Mg^{2+} ions in a critical concentration of 10^{-4} M. Both the Hooge parameter α_H and the equivalent input noise S_U revealed a conductivity increase in the solution concentration range from 10^{-4} M–10^{-1} M. The results are in good agreement with characteristics obtained using the *C–V* technique. The implementation of noise spectroscopy opens up perspectives for analyzing the divalent and multivalent ion dynamic processes and ion–ion correlation effects at the solid-liquid interface for biosensing applications.

4. Experimental Section

The fabrication process for GAA nanowire FET sensors was developed by modifying the technology for complementary metal-oxide-semiconductor (CMOS) devices. The steps involved in the fabrication of nanostructure devices were shown in Figure S2.(Supporting Information) More detailed information is presented below.

We started the clean room (ISO1 standard, stable room temperature [21°C] and humidity [50%–60%]) processing with a 100-orientation SOI substrate (buried oxide layer: ≈150 nm SiO_2, top silicon layer: ≈110 nm Si), the full RCA cleaning had to be performed with a piranha solution (H_2O_2:H_2SO_4 = 2:1) for 10 min, SC-1(NH_4OH:H_2O_2:H_2O = 1:4:20) at 60°C for 10 min, and SC-2(HCl:H_2O:H_2O_2 = 1:20:1) at 60°C for 10 min.

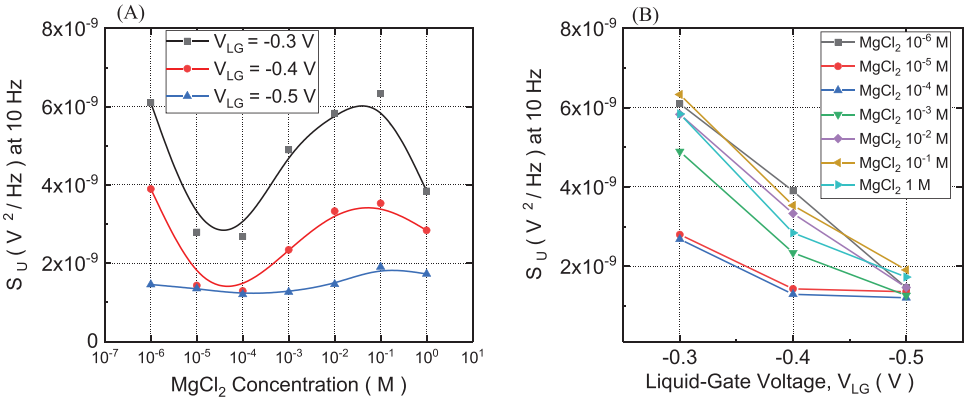

Figure 8. A) The input-referred noise S_U at 10 Hz of NW FETs with a nanowire channel of 2 µm in length and 100 nm in width obtained for different $MgCl_2$ solutions in $V_{DS} = -20$ mV and B) its dependence on V_{LG}.

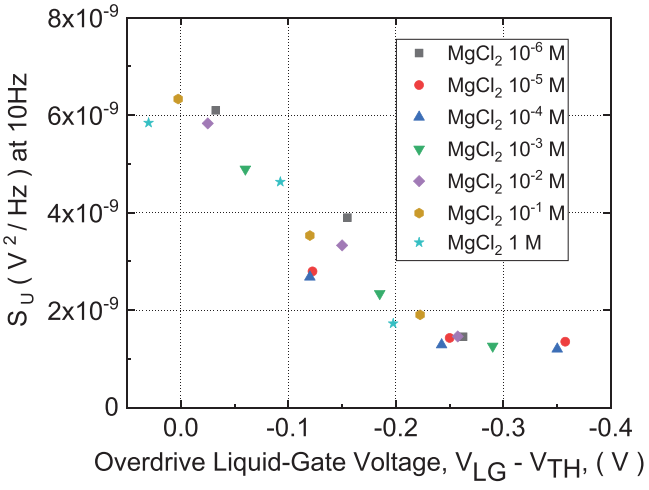

Figure 9. A plot of the input-referred noise S_U at 10 Hz, obtained at different V_{LG} for different $MgCl_2$ concentrations versus the overdrive voltage (V_{LG}–V_{TH}), at $V_{DS} = -20$ mV.

We then typically had to perform dry thermal oxidation of a 20 nm SiO_2 layer at 900°C on the clean SOI surface to form a hard mask. The nanowires and alignment markers were then defined through the SiO_2 surface by spin-coating resists (PMMA and UV-6), soft baking (180°C for 5 min and 130°C for 1 min), electron-beam lithography, and dry etching. To obtain a near-atomic flat nanowire structure on the Si layer, the tetramethylammonium hydroxide (TMAH) solution was applied for wet etching of the Si layer at 80°C. The boron ion implantation was utilized for *P*-type FET sensors, resulting in ohmic contacts: source and drain regions (each region size ≈50 × 100 μm^2). The implemented parameters for energy, dose, and the tilt angle, were 6 keV, 10^{15} cm^{-2}, and 7°, respectively. Moreover, further treatment with rapid thermal annealing (RTA) was performed at 1000°C for 5 s to ensure high-quality ohmic contacts. The 5 nm SiO_2 dielectric layer was obtained using thermal oxidation to cover all nanowire structures. We chose buffered oxide etch (BOE) to open access to the back gate and to create a GAA nanostructure for the convenient measuring of the *I*–*V* characteristics. For the metallization process, 5 nm of Ti and 200 nm of Al were deposited on ohmic contact pads by thermal evaporation, followed by lift-off, and RTP at 450°C for 10 min. Additionally, to protect the device contacts during the measurement, we used a polyimide waterproof layer as the passivation layer via spin coating at 4000 rpm for 60 s (first baking at 110°C for 1 min, then 140°C for 6 min). We subsequently used photolithography to open the windows for nanowires to ensure the access of bioliquids during the *I*–*V* measurements. The samples were then diced to a suitable size and the devices were connected with the chip carrier by Al wire bonds. Finally, we used polydimethylsiloxane (PDMS) to capture sample surfaces with two differently sized rings.

Characterizations: A metal Faraday cage box was used to protect the samples from external electromagnetic radiation during measurements. The Keithley 2400 test system was used to measure the electrical properties of the transistor using *I*–*V* characteristics, with Ag/AgCl as the reference electrode immersed in a bioliquid. For the noise measurements, in-house-developed measurement system with ultralow internal noise was used. As voltage biases were applied to gate-source and drain-source contact during the noise characterization, rechargeable batteries, and potentiometers were used. To ensure voltage stability during measurements, the voltage supply setup needs to be equipped with additional capacitance. The signals of the biosensor were first pre-amplified via an ultra-low in-house-developed noise preamplifier. To further amplify the signal of the sample, the ITHACO 1201 amplifier was used. The signal data were transferred to the computer via the Agilent U2542A simultaneous data acquisition module and a high-speed USB 2.0 interface. The time domain signal was also changed to the frequency domain by a fast Fourier transform. The voltage noise power spectral density (S_V) was recorded in the range of 1 Hz–100 kHz.

Statistical Analysis: A series of FETs were investigated for electrical and noise properties. For electrical properties, the transfer and output curves were studied using the *I*–*V* system. Several nanowire biosensors measuring 100 nm in width and 2 μm in length were used to analyze noise spectra. The original noise data were voltage spectral density, $S_v(f)$, measured as a function of frequency

$$S_v(f) = \lim_{\Delta f \to 0} \frac{(v - \bar{v})^2}{\Delta f} \tag{3}$$

where the mean square voltage fluctuation is $(v\text{-}\bar{v})^2$ in Δf of the frequency band.

The thermal noise due to the charge carrier thermal excitation with thermodynamic fluctuations was taken into account. The voltage variance per hertz of bandwidth of thermal noise is given by:

$$S_{Thermal}(f) = 4KTR_{eq} \tag{4}$$

where K is the Boltzmann constant, T is the non-zero temperature, and R_{eq} is the equivalent resistance.

The spectrum of thermal noise was subtracted from the measured noise spectral, and the formula for the analyzed part of noise is as follows:

$$S_{v,real}(f) = S_v(f) - 4KTR_{eq} \tag{5}$$

For further analysis, the spectral density of current fluctuation was corrected by the formula:

$$S_I(f) = \frac{S_{v,real}(f)}{R_{eq}^2} \left[\frac{1}{1 + \left(\frac{f}{f_0}\right)^2} \right]^{-1} \tag{6}$$

where f_0 is the corner frequency which results from the presence of parasitic capacitance shunting the input of the preamplifier.

Typically, the dimensionless Hooge parameter was used to analyze the noise level for evaluating the performance of the sample using the formula:

$$\alpha_H(f) = \frac{S_I(f)}{V_{DS}^2} \frac{fL^2R}{q\mu_p} \tag{7}$$

where L is the length of the nanochannel, R is the resistance of the device, q is the elementary charge, and μ_p is the mobility of the major carrier (i.e., hole).

For further discussion, the input-referred noise S_U was calculated to describe the ion correlation at the solid/liquid interface at different V_{LG} as follows:

$$S_U(f) = \frac{S_I(f)}{g_m^2} \tag{8}$$

where g_m is the transconductance of a sample extracted from the measured transfer characteristics (*I*–*V*).

Supporting Information

Supporting Information is available from the Wiley Online Library or from the author.

Acknowledgements

Y.Z. and N.B. contributed equally to this work. Y.Z. is very grateful to have received a research grant (No. 202108360085) from the China Scholarship

Council (CSC). The authors would also like to thank all the technical staff at the Helmholtz Nano Facility (HNF) of Forschungszentrum Jülich for their assistance in fabricating the sensor devices. M.P. is very grateful to Helmholtz Fond for their support.

Open access funding enabled and organized by Projekt DEAL.

Conflict of Interest

The authors declare no conflict of interest.

Data Availability Statement

The data that support the findings of this study are available from the corresponding author upon reasonable request.

Keywords

equivalent input noise, GAA (gate-all-around), Hooge parameter, ion behavior, nanowire field-effect transistors, noise spectroscopy

Received: July 7, 2023
Revised: September 10, 2023
Published online:

[1] P. Bergveld, *IEEE Trans. Biomed. Eng.* **1972**, *19*, 342.
[2] F. Patolsky, G. Zeng, O. Hayden, M. Lakadamyali, X. Zhuang, C. M. Lieber, *Natl. Acad. Sci.* **2004**, *101*, 14017.
[3] Y. Cui, Q. Wei, H. Park, C. M. Lieber, *Science* **2001**, *293*, 1289.
[4] H. S. Song, T. H. Park, *Biotechnol. J.* **2011**, *6*, 1310.
[5] N. K. Rajan, D. A. Routenberg, M. A. Reed, *Appl. Phys. Lett.* **2011**, *98*, 264107.
[6] Y. Kutovyi, I. Zadorozhnyi, V. Handziuk, H. Hlukhova, N. Boichuk, M. Petrychuk, S. Vitusevich, *Nano Lett.* **2018**, *18*, 7305.
[7] Y. Kutovyi, I. Zadorozhnyi, H. Hlukhova, V. Handziuk, M. Petrychuk, A. Ivanchuk, S. Vitusevich, *Nanotechnology* **2018**, *29*, 175202.
[8] Y. Kutovyi, H. Hlukhova, N. Boichuk, M. Menger, A. Offenhäusser, S. Vitusevich, *Biosens. Bioelectron.* **2020**, *154*, 112053.
[9] S. X. Li, W. Guan, B. Weiner, M. A. Reed, *Nano Lett.* **2015**, *15*, 5046.
[10] K. B. Parizi, *Sci. Rep.* **2017**, *7*, 41305.
[11] B. I. Shklovskii, *Phys. Rev. E* **1999**, *60*, 5802.
[12] E. Wernersson, R. Kjellander, J. Lyklema, *J. Phys. Chem.* **2010**, *114*, 1849.
[13] D. E. Yates, S. Levine, T. W. Healy, *J Chem Soc.* **1973**, *70*, 1807.
[14] M. Wipf, R. L. Stoop, A. Tarasov, K. Bedner, W. Fu, I. A. Wright, C. J. Martin, E. C. Constable, M. Calame, C. Schönenberger, *ACS Nano Lett.* **2013**, *7*, 5978.
[15] R. Sivakumarasamy, R. Hartkamp, B. Siboulet, J.-F. Dufrêche, K. Nishiguchi, A. Fujiwara, N. Clément, *Nat. Mater.* **2018**, *17*, 464.
[16] Y. Guo, D. Pustovyi, Y. Kutovyi, N. Boichuk, Y. Zhang, S. Vitusevich, *Adv. Mater. Interfaces* **2022**, *9*, 2201142.
[17] A. A. Talin, F. Léonard, B. S. Swartzentruber, X. Wang, S. D. Hersee, *Phys. Rev. Lett.* **2008**, *101*, 076802.
[18] A. A. Talin, F. Leonard, A. M. Katzenmeyer, B. S. Swanentruber, S. T. Picraux, M. E. T Malares, J. G. Gederberg, X. Wang, S. D. Hersee, A. Rishinaramangalum, *Semicond. Sci. Technol.* **2010**, *25*, 024015.
[19] Y. Gu, L. J. Lauhon, *Appl. Phys. Lett.* **2006**, *89*, 143102.
[20] A. D. Schricker, F. M. Davidson, R. J. Wiacek, B. A. Korgel, *Nanotechnology* **2006**, *17*, 2681.
[21] P. Zhang, *J. Appl. Phys.* **2021**, *129*, 10.
[22] S. Alagha, A. Shik, H. E. Ruda, I. Saveliev, K. L. Kavanagh, S. P. Watkins, *J. Appl. Phys.* **2017**, *121*, 17.
[23] K. Besteman, M. A. G. Zevenbergen, S. G. Lemay, *Phys Rev.* **2005**, *72*, 061501.
[24] P. A. Christensenand, A. Hamnett, *Techniques and Mechanisms in Electrochemistry*, Blackie Academic & Professional, An Imprint Of Chapman & Hall, Kluwer Academic Publishers, Glasgow **1994**, 379.
[25] H. Hlukhova, *MRS Adv.* **2018**, *3*, 1535.
[26] F. N. Hooge, *Phys. Lett.* **1969**, *29*, 139.
[27] M. Hartman, M. Östling, *Low-Frequency Noise in Advanced MOS Devices*, Springer, Berlin **2007**, 216.
[28] J. Lee, I. Han, B.-Y. Yu, G.-C. Yi, G. Ghibaudo, *J Korean Phys Soc* **2008**, *53*, 339.
[29] E. Niklas, R. J., I. Sychugov, T. Engfeldt, A. E. Karlstrom, J. Linnros, *Nano Lett.* **2007**, *7*, 2608.
[30] J. Li, S. Pud, D. Mayer, S. Vitusevich, *Nanotechnology* **2014**, *25*, 275302.
[31] J. Li, *J. Appl. Phys.* **2013**, *114*, 20.
[32] M. J. Kirton, M. J. Uren, *Adv. Phys.* **1989**, *38*, 367.
[33] Y. Shen, J. Cui, S. Mohammadi, *Solid-State Electron.* **2017**, *131*, 45.
[34] M. Kuscu, O. B. Akan, *IEEE Trans. Commun.* **2016**, *64*, 3708.
[35] M. Petrychuk, I. Zadorozhnyi, Y. Kutovyi, S. Karg, H. Riel, S. Vitusevich, *Nanotechnology* **2019**, *30*, 305001.
[36] Y. Kutovyi, I. Z., H. Hlukhova, M. Petrychuk, S. Vitusevich, *IEEE* **2017**, 7986024.
[37] F. Najam, Y. S. Yu, K. H. Cho, K. H. Yeo, D.-W. Kim, J. S. Hwang, S. Kim, S. W. Hwang, *IEEE Trans. Electron Devices* **2013**, *60*, 2457.